

## Electronic properties of small supported Pt particles: NMR study of $^{195}\text{Pt}$ hyperfine parameters

J. P. Bucher and J. J. van der Klink

*Institut de Physique Expérimentale, Ecole Polytechnique Fédérale de Lausanne, CH-1015 Lausanne, Switzerland*

(Received 16 May 1988)

A combination of Knight-shift and relaxation-time measurements ( $K, T_1$ ) in small Pt particles allows a quantitative interpretation in terms of the local densities of states (LDOS) at the Fermi energy for the  $s$ -like and  $d$ -like electrons. The definite metallic character of our Pt particles, evidenced by the Korringa relationship, allows us to describe  $K$  and  $T_1$  by well-known equations for metals. We have included additional factors to take into account site-dependent Stoner enhancement effects. This description establishes the correspondence:  $(K, T_1) \rightarrow (D_s(E_F), D_d(E_F))$ . We find a depleted Fermi LDOS along with a significant de-enhancement of the clean surface with respect to the bulk, due essentially to  $d$  electrons. We discuss the hydrogen-adsorbate-induced modification of the surface Fermi LDOS at  $E_F$  which is further diminished compared to the clean one. As a byproduct of this analysis, we obtain the susceptibility of an assembly of small particles (mean particle size 27 Å):  $\chi/\chi_{\text{bulk}} = 0.6$  at 20 K. This work also presents a contribution to the problem of metal-support interactions which may become important in Pt/TiO<sub>2</sub> systems when reduced above 500 °C.

### I. INTRODUCTION

For many years, magnetic resonance work on small metal particles has been done with a view to putting forth the discrete nature of energy levels near the Fermi energy. However, the Pt nuclear-magnetic-resonance experiments of Slichter and co-workers<sup>1,2</sup> on Pt catalysts showed that surface effects due to the large surface-to-volume ratio prevail over pure quantum size effects, even for particles as small as 20 Å. In this work, we show that hyperfine field interaction parameters, as provided by NMR observables, are a suitable tool to investigate local electronic properties of those small Pt particles. Although NMR spectra combined with relaxation-time measurements are known to give reliable information on the local structure in metals and alloys,<sup>3</sup> it was not clear at the outset how to interpret NMR data of small particles, in order to get quantitative information such as local densities of states (LDOS) at the Fermi energy  $E_F$ . In this work, we give one possible interpretation in terms of the most probable solid-state approach corroborated by the metallic character of surface nuclei relaxation. Extending the work of Yafet and Jaccarino,<sup>4</sup> we have developed a parametrization scheme<sup>5</sup> based on a two-band model: many-body effects are taken into account separately for the  $5d$  and the  $6s$  band by means of a Stoner-like description. The site-dependent formulation, imposed by the reduced symmetry and coordination of surfaces, follows by making some plausible assumptions. In this way, adsorbate-induced modifications of the electronic structure at metal surfaces can also be studied for different metal-adsorbate systems. Moreover, when metal-support interactions are induced, information can be gained on the interface.

In recent years, hyperfine field interactions have been studied theoretically to a large extent,<sup>6,7</sup> motivated by

speculation about some new magnetic properties of transition-metal surfaces. Some results allow advantageous comparisons with the experiments on small particles. Therefore, new insights will undoubtedly be gained from interplay between experiment and theory.

A real advantage of NMR over conventional methods widely used in surface science [various electron spectroscopies, low-electron electron diffraction (LEED) Auger, etc.] is that the samples may be studied at their usual working pressure (mostly above  $10^{-2}$  bar), rather than in ultrahigh vacuum with samples having as high a surface area as possible instead of the flat surface of single crystals. In this respect, NMR is very promising in making a bridge between the fundamental surface science approach and catalysis research.

We have chosen TiO<sub>2</sub> rather than SiO<sub>2</sub> (Ref. 8) as a support material. This choice leads to an improvement of the signal-to-noise ratio, since for the same surface area of the support, available TiO<sub>2</sub> was shown to be much more compact than SiO<sub>2</sub> or Al<sub>2</sub>O<sub>3</sub>. In addition, the Pt/TiO<sub>2</sub> system provides a unique opportunity for studying in some detail the so-called "strong metal-support interaction" effect (SMSI). Actually, SMSI was the name given to a remarkable change in hydrogen chemisorption capacity for Pt on TiO<sub>2</sub> after high-temperature reduction<sup>9</sup> (HTR) as compared to after a low-temperature reduction (LTR), discovered some ten years ago. The phenomenon was found to be reversible under reoxidation and low-temperature reduction (RR). It should be mentioned that Tauster *et al.*<sup>9</sup> also demonstrated that trivial explanations of the SMSI phenomenon, such as sintering or massive encapsulation of the metal (by the support), may be ruled out on general experimental grounds. Although Pt/TiO<sub>2</sub> is not the only system showing SMSI,<sup>10</sup> it is the most studied. Later, it was found that other catalysts [e.g., Pt/Al<sub>2</sub>O<sub>3</sub> (Ref. 11) and Pt/SiO<sub>2</sub>

(Ref. 12)] also lose their chemisorption capacity when treated at sufficiently high temperature. Reduction of the support has been suggested for the Pt/Al<sub>2</sub>O<sub>3</sub>,<sup>13</sup> and even formation of intermetallic compounds has been reported for the Pt/SiO<sub>2</sub> system.<sup>14</sup>

## II. SAMPLE PREPARATION AND CHARACTERIZATION

The samples consist of small Pt particles (a few nanometers in diameter) supported on slightly bigger grains of TiO<sub>2</sub>-anatase, 180 m<sup>2</sup>/g from Bayer (a few tens of nanometers in diameter). They were prepared via reduction of hexachloroplatinate in an aqueous solution following the method described elsewhere.<sup>15</sup> In this technique, the particles are preformed in the colloidal solution prior to deposition on the support. This procedure minimizes the metal-support interaction that occurs inevitably in other techniques of preparation, such as pore impregnation or ion exchange, where an intimate contact between support and the metal precursor is a necessary condition. The SMSI effect is only triggered upon reduction above 500°C, whatever the method of preparation. The Pt 4f<sub>5/2</sub> and 4f<sub>7/2</sub> XPS lines of our powder sample occurred at positions expected for metallic Pt, indicating complete reduction of the Pt particles. The Pt loading of our sample is 3.8 at. %, as determined by spectrophotometric measurements following Ayre's method,<sup>16</sup> after forming the (PtSn<sub>4</sub>Cl<sub>4</sub>)<sup>4+</sup> complex in solution.

In the fields of catalysis, samples are characterized by their Pt dispersion which is defined as the fraction of Pt atoms on the surface. For different reasons, experimental determinations of this idealized notion of dispersion are only approximate. We have used hydrogen chemisorption<sup>15</sup> and high-resolution transmission electron microscopy (TEM). In the first method, the dispersion is calculated from the hydrogen uptake (one monolayer) and from the Pt mass content of the sample. In the second method, the dispersion is calculated from the particle size distribution (Fig. 1) assuming that the particles have a cubooctahedral shape.<sup>17</sup> The electron micrographs were taken with a Philips 300S apparatus.

It was first suggested by Rhodes *et al.*<sup>1</sup> that NMR can also provide a measure of the dispersion, since surface atoms give a distinct signal at the low-field end of the spectrum. Experimentally, the high- and low-fields ends are not well separated. We have to make an assumption about the low-field "line shape;" we take it as symmetric. Then, the ratio of the area of the symmetrical low-field line over the total area of the total line gives a measure of the dispersion. The validity of the procedure is, however, restricted to "clean" samples (no adsorbates); see also Ref. 15. Dispersion measurements are summarized in Table I. Electron microscopy and NMR results are in good agreement. The higher value obtained by chemisorption is not surprising, since hydrogen chemisorption tends to overestimate the dispersion of Pt particles supported on oxides, as was shown in a systematic study.<sup>15</sup>

After synthesis, the samples were treated with a view to NMR analysis. A universal all-glass apparatus coupled to a turbomolecular pump allows us to further clean

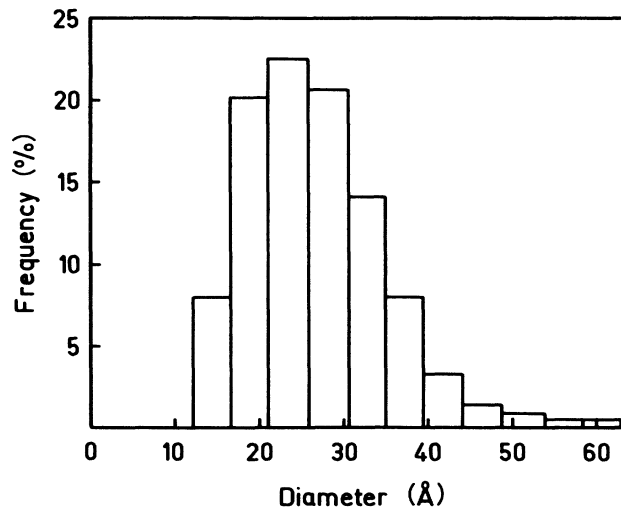


FIG. 1. Particle-size distribution as deduced from TEM. The sample population was 700. The mean diameter is 27 Å.

the powder samples and to perform the final H reduction at various temperatures. In addition, it is possible to adsorb a well-defined gas on the Pt particles before sealing the sample in a glass ampoule.

We have studied four different samples from the same batch, which have undergone different treatments. The standard procedure is summarized in Table II for the sample reduced at low temperature (LTR). In the case of the sample reduced at high temperature (HTR), the reduction was done at 500°C and the values which have to be considered, following Tauster *et al.*<sup>9</sup> are given in parentheses. After the treatment, these samples were cooled under a continuous He flow and sealed in a glass ampoule with a controlled atmosphere of 0.5 bar He gas.

In order to test the assumption of some authors that the SMSI effect would be due to hydrogen back spillover from the support, we also prepared a sample (LTRH) reduced at low temperature and subsequently covered with hydrogen. The back-spillover hypothesis supposes that during the cool down after HTR, the support releases hydrogen stored during the treatment so that the metal becomes covered with hydrogen, which prevents a further hydrogen adsorption.<sup>18</sup> The treatment is the same as for the LTR sample, except that after reduction at 200°C the sample was allowed to cool down to room temperature under a constant H<sub>2</sub> flow; then the excess hydrogen was pumped and the sample was sealed with a controlled atmosphere of 0.5 bar He gas. In that way, we expect the H coverage to be most nearly one monolayer.

In order to also test the reversibility of the SMSI effects from the NMR point of view, we prepared a rereduced

TABLE I. Platinum dispersion measurements.

Method	Dispersion (%)
H <sub>2</sub> chemisorption	50
Electron microscopy	36
NMR	37

TABLE II. Standard treatment of Pt/TiO<sub>2</sub> samples. The samples are first evacuated for 20 h, while temperature was increased from ambient to 300°C. Oxidation and reduction were done at a pressure of 1 bar. The pumping steps were done at better than 10<sup>-6</sup> mbar. Values in parentheses refer to preparation of the SMSI state (see text).

	Flow (ml/min)	Temperature (°C)	Time (h)
pumping		0–300	20
O <sub>2</sub>	20	300	1
He	200	300	0.25
pumping		300	1
pumping		300–200 (300–500)	
H <sub>2</sub>	50	200 (500)	1
(H <sub>2</sub> )	(50)	(500–450)	
He	200	200 (450)	0.25
pumping		200 (450)	1
(pumping)		(450–200)	
He	50	200–20	
sealing			

sample (RR), where RR means the following steps: HTR/O<sub>2</sub>, 400°C, 1 h/LTR. As was shown by Tauster *et al.*, this treatment restores the full ability of the catalyst to adsorb hydrogen.

Our bulk Pt reference sample was prepared by reducing a mixture of PtO<sub>2</sub> (Adam's catalyst, Fluka) and Al<sub>2</sub>O<sub>3</sub> in hydrogen at 300°C for 2 h. This results in fine insulated Pt grains of about 10 μm, having bulk properties.

### III. NMR EXPERIMENTAL METHOD

The NMR equipment is composed of an Oxford 8 T superconducting magnet and a home-made pulsed NMR spectrometer with quadrature detection. The experiment, made up of different instruments, is driven by a Hewlett-Packard 9816 microcomputer through the HP-IB bus. The software manages the whole NMR experiment and allows extensive data manipulations. The system controls the pulse programmer with its own on-board memory [48 bits wide, 1 kbyte long (2<sup>10</sup>=1024)] using TTL circuitry to achieve maximum speed. The 1024 steps, with appropriate looping, enable complicated pulse sequences to be generated, as is required by the important signal averaging needed in Pt particle NMR. Signal averaging takes place in a two-channel accumulator on the supervision of the pulse generator: the quadrature signal passes through two AD converters of either 8 bits (maximum sampling frequency 10 MHz) or 12 bits (maximum sampling frequency 500 kHz) and is stored, according to an eight-phase add-subtract scheme, into a memory of 16 bits wide and 4096 long.

The spectra were measured point by point by a frequency-swept spin-echo technique ( $\pi/2$ - $\tau$ - $\pi$ - $\tau$ -echo) between 69.5 and 74.0 MHz. The separation  $\tau$  between the  $\pi/2$  and the  $\pi$  pulses was 35 μs, while the length of the  $\pi/2$  pulse was 5 μs. The spin-lattice relaxation time was measured by recording the recovery of the spin-echo intensity after a saturation comb. The feasibility of the technique was tested on our Pt bulk sample. We found

$T_1 T = 0.0296 \pm 0.0010$  (s K) at 77 K which is very close to the tabulated value of  $T_1 T = 0.013$  s K.<sup>3</sup>

The official reference for the zero Knight shift for Pt is H<sub>2</sub>PtI<sub>6</sub>. However, this compound is unstable and therefore difficult to obtain. One prefers generally to work with H<sub>2</sub>PtCl<sub>6</sub>. Since the chemical shift of H<sub>2</sub>PtCl<sub>6</sub> with respect to H<sub>2</sub>PtI<sub>6</sub> is known,  $\delta = 6300$  ppm,<sup>19</sup> it is easy to make the conversion.

### IV. EXPERIMENTAL RESULTS

We have observed <sup>195</sup>Pt NMR signals in all four samples described in Sec. III (Fig. 2). Some characteristics of NMR in small Pt particles have already been mentioned in a previous paper.<sup>8</sup> Therefore, we only recall some general features based on the example of the clean LTR sample [Fig. 2(a)], where the particles are supposed to have negligible interaction with the support. The resonance line is shown to be very broad. This is the common situation for the particle sizes encountered here (mean diameter 27 Å, Fig. 1). The signal extends from below the characteristic "surface peak" at the low-field end, close to the conventional zero-Knight-shift position, to beyond the position of the bulk signal, with a Knight shift of about -3.44%.<sup>3</sup>

All our spectra were corrected for spin-spin ( $T_2$ ) relaxation-time effects. This correction also accounts for additional oscillatory behavior of the spin-echo envelope due to indirect spin-spin coupling.<sup>20</sup> The corrections were made on the basis of separate  $T_2$  measurements across the spectra for all our samples. They affect the measured amplitude differently at high and low fields. As a guideline for further measurements, the correction of the signal amplitude can be taken to be linear across the line, with no correction for the low-field end ( $H_0/\nu_0 = 1.100$  G/kHz), the high-field end ( $H_0/\nu_0 = 1.137$  G/kHz) being 20% more intense for  $\tau = 35$  μs.

The spectrum of the LTR sample [Fig. 2(a)] is not significantly different from that of samples of the same particle sizes prepared on "nonreducible" oxides such as SiO<sub>2</sub> (see, for instance, sample No. 1 of Ref. 8). Therefore, NMR results on clean particles obtained by the colloidal route indicate a very limited influence of the support, as long as no HTR has been done.

The spectra in Fig. 2 show various treatments, and they are all normalized to the same area under the line. As is shown in Fig. 2(a), HTR has a tremendous effect on the line shape. The surface peak does not shift appreciably upon HTR, but increases in amplitude at the expense of the bulk peak, indicating that after HTR treatment fewer nuclei are in bulklike sites. The Pt NMR line shape for the RR sample is shown in Fig. 2(b) (solid triangles). These points are superposed very well on the line obtained for the LTR sample (dashed line); the SMSI effect is fully reversible, also from the NMR point of view. That the surface obtained after HTR is not a simple hydrogen-covered one [Fig. 2(c)] follows from the surface peak position of the LTRH sample and, still more convincingly, from relaxation times.

In Fig. 3, we present nuclear spin-lattice relaxation times measured across the resonance lines. In the

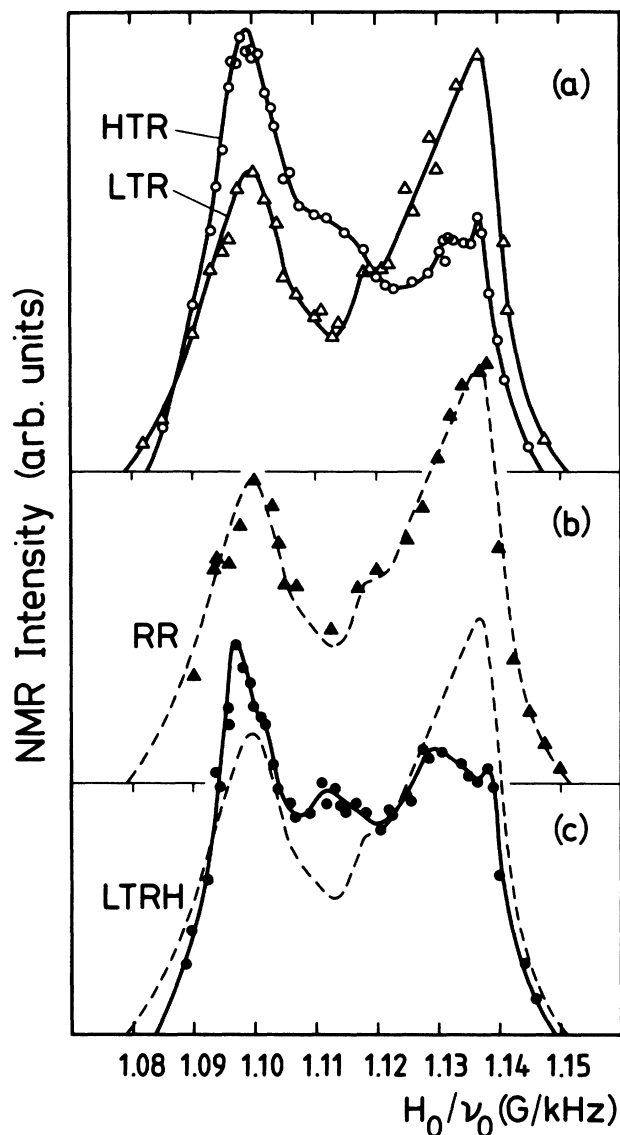


FIG. 2.  $^{195}\text{Pt}$  NMR spectra for the LTR, HTR, RR, and LTRH samples, measured by the frequency-swept spin-echo method at 20 K ( $H_0 = 8$  T). (a) LTR and HTR samples: open triangles and open circles, respectively. The characteristic features are the “surface” peaks, at the low-field end  $H_0/\nu_0 = 1.0995$  G/kHz, and the “bulk” peaks at the high-field end  $H_0/\nu_0 = 1.1370$  G/kHz. Note that there is no shift of the peaks (within experimental errors) upon HTR. (b) RR sample: solid triangles. By way of comparison, the dashed line shows the original LTR sample. This overall agreement demonstrates the complete reversibility under RR. (c) LTRH sample: solid circles. For comparison, the clean HTR sample is also shown (dashed line). A remarkable fact is that hydrogen coverage produces a small shift of the surface peak to a value of  $H_0/\nu_0 = 1.097$  G/kHz.

Knight-shift range from the “bulk” position ( $H_0/\nu_0 = 1.137$  G/kHz)—where the values of  $T_1$  agree well with  $T_1$  in a bulk sample—to about  $H_0/\nu_0 = 1.110$  G/kHz, all three samples show a similar  $T_1$  variation. This expresses the fact that nuclei resonating at these frequencies are in a very similar environment. Meanwhile,

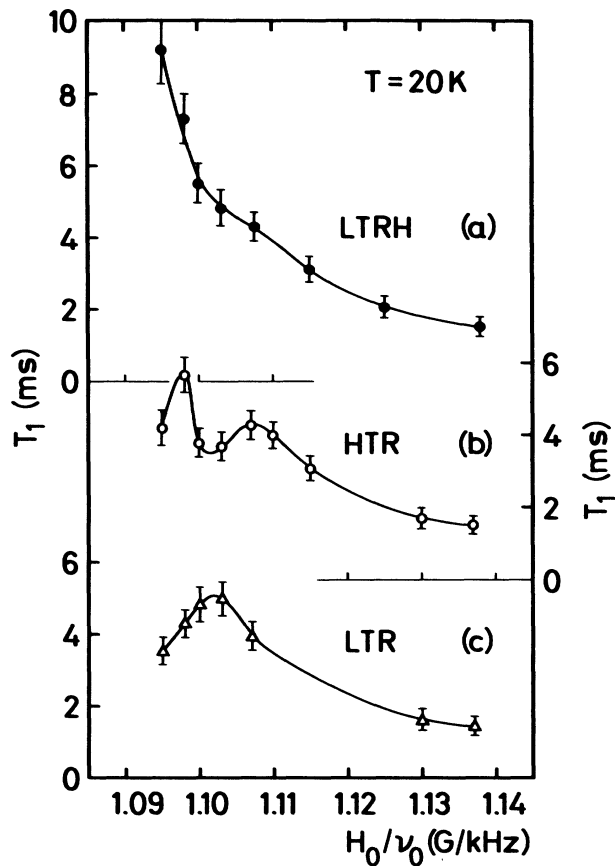


FIG. 3. Spin-lattice relaxation times as a function of  $H_0/\nu_0$  measured by the saturation technique at  $T = 20$  K. The lines are only a guide for the eyes. The error bars enter directly into the calculation of the bare density of states.

the picture becomes very different around  $H_0/\nu_0 = 1.100$  G/kHz.

Nuclei resonating in the surface peaks of three different samples (LTR, HTR, LTRH) have clearly different relaxation times. This indicates that the sample treatment affects the electronic structure at the surface (cf. Sec. V). The order of magnitude of the relaxation times stays comparable to that of the bulk metal (and is very different from that of diamagnetic compounds), hinting at a probable metallic character of the surface. Definite evidence for this metallic character is shown in Fig. 4, where we have reported  $T_1^{-1}$  as a function of the temperature  $T$  for the surface resonance of the LTR, HTR, and LTRH samples. The straight lines indicate that the relaxation obeys a Korringa relation,<sup>21</sup> or, in other words, that relaxation of surface nuclei is governed by conduction electrons.

## V. DATA ANALYSIS

As a starting point in the analysis of the NMR data we will adopt the equations for  $K$  and  $T_1$  proposed by Yafet and Jaccarino,<sup>4</sup> but we include additional factors<sup>22</sup> to take into account Stoner enhancement effects.<sup>23</sup> We have shown<sup>5</sup> that such equations can represent very well the experimental data for the spin susceptibility  $\chi$ , the

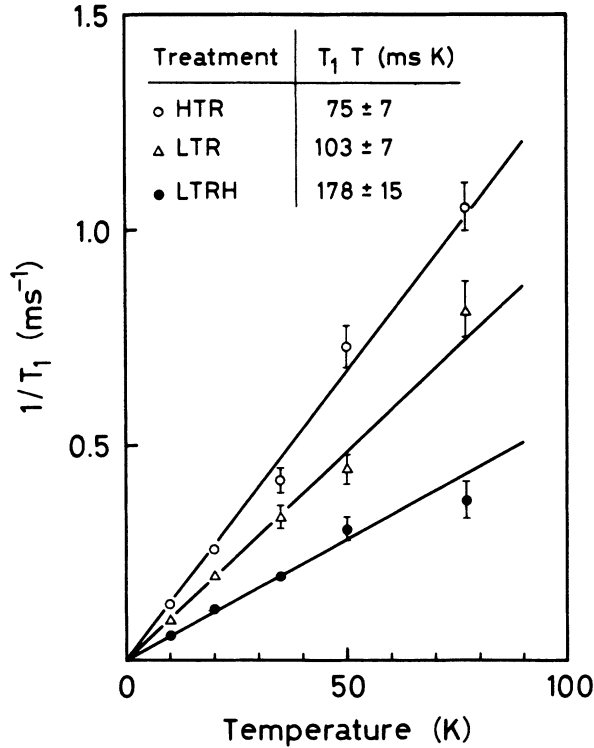


FIG. 4.  $T_1^{-1}$  as a function of temperature measured at the positions  $H_0/\nu_0 = 1.100$  G/kHz for LTR and HTR samples and  $H_0/\nu_0 = 1.098$  G/kHz for the LTRH sample. The straight lines are indicative of a conduction-electron type of relaxation.

Knight shift  $K$ , and the relaxation rate  $T_1^{-1}$  in bulk Pt (including their temperature variation) and reasonably well those for bulk Pd. The equations adopted for the data analysis are

$$\chi = \frac{1}{1-\alpha_s} \mu_B^2 D_s(E_F) + \frac{1}{1-\alpha_d} \mu_B^2 D_d(E_F) + \chi_{\text{orb}}, \quad (1)$$

$$K = \frac{1}{1-\alpha_s} \mu_B D_s(E_F) H_{\text{hf},s} + \frac{1}{1-\alpha_d} \mu_B D_d(E_F) H_{\text{hf},d} + K_{\text{orb}}, \quad (2)$$

$$S(T_1 T)^{-1} = k(\alpha_s) K_s^2 + k(\alpha_d) K_d^2 R_d + [\mu_B D_d(E_F) H_{\text{hf},\text{orb}}]^2 R_{\text{orb}}, \quad (3)$$

where  $D(E_F)$  is the bare density of states at the Fermi energy,  $\alpha$  represents the Stoner factor for the static susceptibility, and  $k(\alpha)$  corrects for the difference in exchange enhancement between  $K^2$  and  $(T_1 T)^{-1}$ ,<sup>23</sup> the  $H_{\text{hf}}$  are hyperfine fields, and the indices  $s$ ,  $d$ , and  $\text{orb}$  indicate contributions from the two bands and the orbital contribution.  $R_d$  and  $R_{\text{orb}}$  are reduction factors and arise from the orbital degeneracy.<sup>4</sup> The  $\alpha$ 's can be expressed as

$$\alpha_\lambda = I_\lambda D_\lambda(E_F), \quad \lambda = s, d \quad (4)$$

where  $I$  is an appropriate exchange integral.

In the bulk,  $I_d$ ,  $I_s$ , and  $H_{\text{hf},s}$  are considered to be freely fittable parameters; excellent agreement between experi-

TABLE III. Parameters appearing in Eqs. (1)–(3) as appropriate for bulk Pt. The indicated error margins are introduced to reflect some uncertainty in their applicability to the small-particle case.

Hyperfine fields	
$H_{\text{hf},d}$ ( $10^6$ G)	$-1.18^a$
$H_{\text{hf},s}$ ( $10^6$ G)	$2.7 \pm 0.5^b$
$H_{\text{hf},\text{orb}}$ ( $10^6$ G)	$1.18 \pm 0.20^c$
Exchange integrals	
$I_d$ (mRy)	$37.7^b$
$I_s$ (mRy)	$98 \pm 5^b$
Reduction factors	
$R_d$	$0.21^{a,d}$
$R_{\text{orb}}$	$0.87^{a,d}$
Densities of states	
$D_s(E_F)$ ( $\text{Ry}^{-1} \text{at.}^{-1}$ )	$4.08^e$
$D_d(E_F)$ ( $\text{Ry}^{-1} \text{at.}^{-1}$ )	$20.4^e$

<sup>a</sup>Reference 58.

<sup>b</sup>Reference 5.

<sup>c</sup>Reference 22.

<sup>d</sup>Reference 59.

<sup>e</sup>Reference 60.

mental values and those found from Eqs. (1)–(3) is obtained using the parameters given in Table III and the  $k(\alpha)$  relationship given by Shaw and Warren.<sup>23</sup>

The lower symmetry of the Pt nuclear sites in small particles creates two changes with respect to the bulk: first, Eqs. (1)–(3) should be replaced by anisotropic variants, and second, all parameters become site dependent. Experimentally, one has no direct access to the local susceptibility [Eq. (1)], since CESR measurements only give a particle-average value; and in a general way the results of total susceptibility measurements in small particles tend to be controversial.<sup>24</sup> We must therefore eliminate Eq. (1) from our considerations.

In a limiting case, each and every Pt nucleus in a particle would give rise to a distinct, relatively sharp NMR line with its own characteristic Knight shift. The observed spectrum is then the envelope of many such “discrete” spectra due to different particles. Indeed, we find from  $T_2$  measurements that the homogeneous linewidth (for a given, “well-defined” site) is of the order of  $10^{-3}$  times the width of the observed spectrum. Strictly speaking, therefore, a given position in the observed spectrum is not necessarily associated with one single site in a certain size of particle: we must interpret it in some “powder-average” (“most-likely-site”) way. Experimentally, we find that the observed  $T_1$  does not vary much when shifting the frequency a few times the homogeneous linewidth; therefore we neglect anisotropies, and assume that the relation between relaxation time  $T_1$  and position in the line (parametrized by  $K$ ) is still given by Eqs. (2) and (3).

As a second simplifying assumption, we will consider only the local densities of state  $D_s(E_F)$  and  $D_d(E_F)$  as site dependent, and keep all other parameters in Eqs. (2)

and (3) as equal to the values used to fit the bulk data.<sup>5</sup> (We will briefly discuss another choice of site-dependent parameters later in this section.) The justification for the latter is that the hyperfine fields are most nearly atomic properties, and that  $I$  [Eq. (4)] is an integral property. Indeed,  $H_{hf,d}$  has been shown to be fairly independent of local environment,<sup>7</sup> and one expects the same to hold for

$H_{hf,s}$ . As we will show in Sec. IV, the local susceptibilities and local densities of state at the Fermi energy given by Weinert and Freeman<sup>7</sup> can be interpreted as evidence in the favor of a site-independent value for the exchange integral. Similarly, the temperature variation of the Korringa relation in the bulk can be fitted by letting  $D_d(E_F)$  in Eqs. (1)–(3) be effectively temperature dependent, keeping all other parameters constant. A somewhat related observation has been made from band-structure calculations for bulk metals:<sup>25</sup> across the transition series of metals,  $D(E_F)$  may change one order of magnitude while  $I$  at the same time changes a few percent.

Under these assumptions, each of the experimental

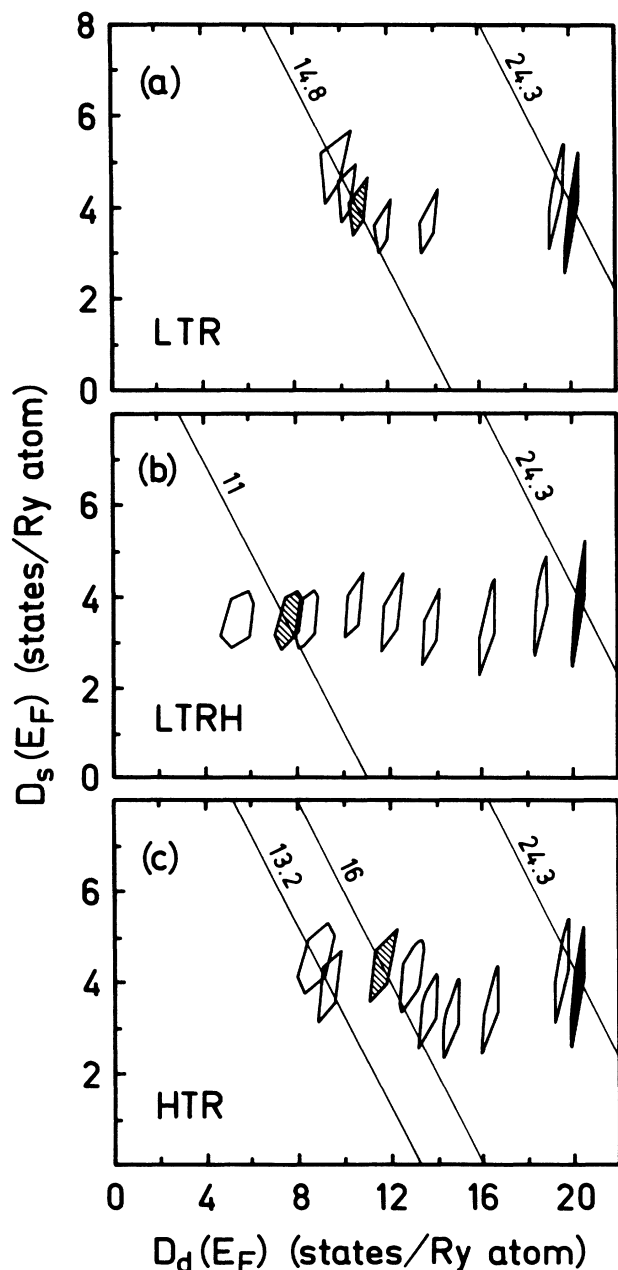


FIG. 5.  $D_s(E_F)$  vs  $D_d(E_F)$  as calculated from the points in Fig. 3 and the values in Table III. The polygons indicate the uncertainty domains. The hatched areas correspond to the surface peaks and the solid ones to the bulk position. (a) LTR sample. (b) LTRH sample. (c) HTR sample. The straight lines indicate total LDOS values for some specific points. The dashed area for the LTRH sample is not from direct measurement at the surface position, but is interpolated from Fig. 4.

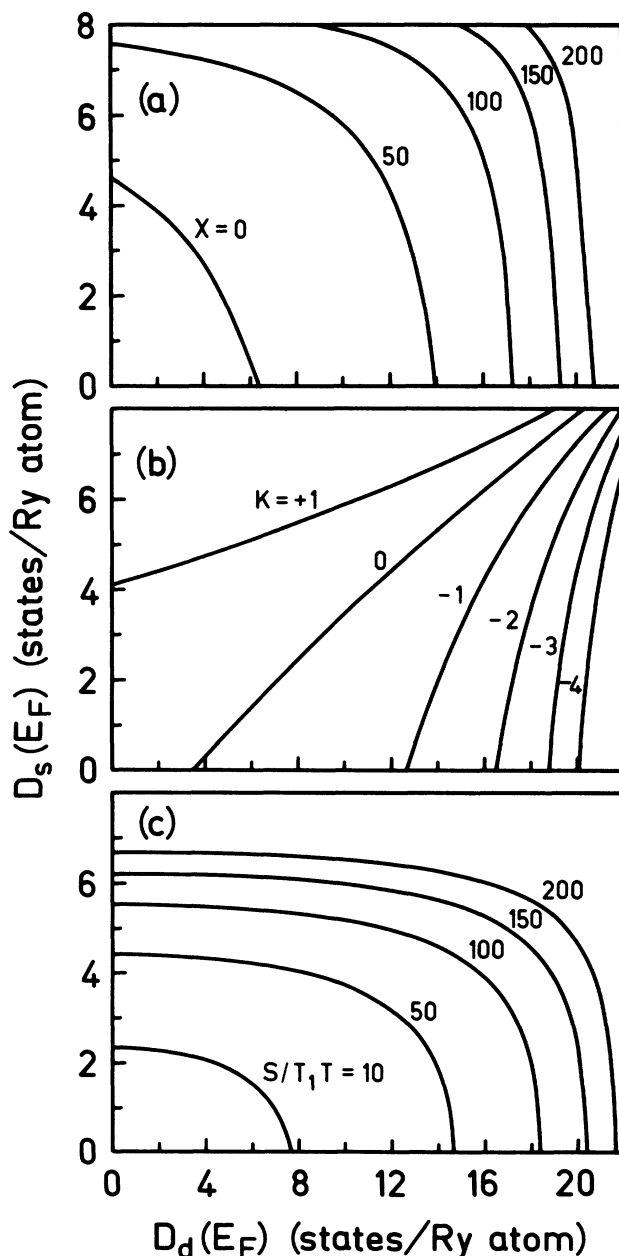


FIG. 6.  $D_s(E_F)$  as a function of  $D_d(E_F)$  for various values of (a) the susceptibility  $\chi$  ( $10^{-6}$  emu/mol); (b) the Knight shift  $K$  (%); (c)  $S/T_1 T$  ( $10^{-6}$ ).

TABLE IV. Whole set of data as obtained from our analysis for the bulk (solid area in Fig. 5) and the surfaces (hatched in Fig. 5).

	$\alpha_d$	$\alpha_s$	$K_d$ (%)	$K_s$ (%)	$K_{orb}$ (%)	$K$ (%)	$(S/T_1T)_d$ ( $10^{-6}$ )	$(S/T_1T)_s$ ( $10^{-6}$ )	$(S/T_1)_{orb}$ ( $10^{-6}$ )	$(S/T_1T)_{tot}$ ( $10^{-6}$ )
Bulk	0.77	0.38	-4.38	0.72	0.21	-3.45	110	35.5	40.5	186
Surface										
LTR	0.41	0.38	-0.93	0.71	0.21	-0.01	11.7	34.9	11.6	58.2
HTR	0.44	0.41	-1.05	0.84	0.21	0.0	14.4	45.7	13.4	73.5
LTRH	0.30	0.35	-0.58	0.64	0.21	0.27	5.2	28.9	6.3	40.4

points in the  $T_1$  versus  $K$  relation implicit in Fig. 3 is reduced to a point in a  $D_s(E_F)$  versus  $D_d(E_F)$  relation as shown in Fig. 5. The polygons indicate the uncertainty domains. The hatched areas correspond to the surface peaks and the solid ones to the bulk position. In Table IV we show the whole set of data available from our analysis for some specific points.

To illustrate the relation between Eqs. (1)–(3) and the  $D_s(E_F)$ - $D_d(E_F)$  plane as used in Fig. 5, we have drawn contours of constant susceptibility  $\chi$ , constant Knight shift  $K$ , and constant normalized relaxation rate  $S/T_1T$  on the same plane in Fig. 6 (contours of constant total density of states are of course just simple straight lines). The points in Fig. 5 can each be considered as an intersection of a  $K$  and a  $T_1$  contour corresponding to the data in Fig. 3.

We have also tried to fit the data of Fig. 3 by allowing  $I_d$  and  $D_d(E_F)$  to vary across the line, keeping all other parameters at their bulk value. As expected from the weak variations in  $D_s(E_F)$  across the line in Fig. 5, this gives very similar results [for  $I_d$  and  $D_d(E_F)$ ] as in the  $D_s(E_F)$ - $D_d(E_F)$  fit. In our further discussion we will only refer to the latter.

## VI. INTERPRETATION OF THE RESULTS

Even if the simplifying assumptions in Sec. V left us with systems of two equations [for  $K$  and  $(T_1T)^{-1}$ ] with two unknowns [ $D_d(E_F)$  and  $D_s(E_F)$ ], it is not a trivial fact that they can be solved for physically realistic values at all, given the nonlinearity of the equations. Therefore, we feel that the gross features of the local densities of state (in Fig. 5), together with the information on the relative number of sites that have such an LDOS (implicit in Fig. 2), represent a useful approximation to the actual situation.

Contrary to the geometry-based model of Makowka *et al.*,<sup>2</sup> we will distinguish only a “bulklike” and a “surface-like” region. Actually, little is known about the surface geometry of supported particles as occur in catalysts. In one study,<sup>26</sup> platinum was shown to keep its fcc structure for particles as small as 15 Å and to adopt cubooctahedral shapes. One generally supposes an equipartition of low index surface planes of the type (111) and (100) for particles of the size concerned in this work, although this assumption has never received a conclusive experimental confirmation. For cubooctahedra of sizes below 20 Å, edge and corner sites become dominant. Surface reconstruction may further complicate the problem. From all

these considerations, it follows that the concept of surface statistics is something very loose in a real catalyst. We will therefore use “surface” in a rather general sense (consistent with the “powder-average” interpretation of our data), even if occasionally we make comparisons with the results of surface studies on specific single-crystal planes. From the negative value of the core-polarization hyperfine field  $H_{hf,d}$  (Table III) it becomes clear why surface nuclei can have a “metallic” type of relaxation [Eq. (3)] although they experience an almost zero shift [Eq. (2)].

As has been mentioned before, the  $K$ - $T_1$  relation [and therefore also the  $D_d(E_F)$ - $D_s(E_F)$  relation obtained from our analysis] in the bulklike region of the spectrum is the same in all samples, including a bulk one. It follows from Fig. 2 that the fraction of atoms in a bulklike environment decreases when going from the LTR to the LTRH to the HTR treatment; and that it is restored by the HTR-reoxidation-LTR sequence (denoted RR in Fig. 2).

All treatments (LTR, HTR, LTRH) result in a total LDOS [ $D_s(E_F) + D_d(E_F)$ ] at the surface that is lower than that in the bulk, the biggest part of the variation being due to  $D_d(E_F)$  [in fact, as remarked in Sec. V, the data can also be fitted reasonably well by constraining  $D_s(E_F)$  to be fixed]. The relative constancy of  $D_s(E_F)$  throughout the spectra then indicates that the geometric boundary effects<sup>2,24</sup> affect the  $s$  electrons in only a negligible fraction of the sites for this size of particles. Similar indications come from the oscillatory behavior of the spin-echo envelope measured in a  $T_2$  experiment: we observed the same beat frequency at surface and bulk positions. This implies the same Ruderman-Kittel coupling constant and consequently the same  $s$ -LDOS at  $E_F$ .<sup>5</sup>

### A. The clean surface (LTR)

As shown in Table I, the relative areas of bulk and surface signals [LTR in Fig. 2(a)] correlate well with dispersion values derived from electron micrographs. The change of the surface LDOS with respect to the bulk [Fig. 5(a)] can easily be explained with a tight-binding argument for the  $d$  band:<sup>27</sup> the width of the  $d$  band is proportional to the square root of the coordination number (for a bulk fcc structure, this number is 12 and may drop down to 5 for a corner atom in a cubooctahedral particle). Then, considering the LDOS at the “clean” surface and supposing for the moment that the center of gravity of the band does not shift, the Fermi energy will cut through the high-end tail of the band where the DOS is

TABLE V. Stoner enhancement as calculated from Weinert and Freeman's data. Comparison with our own results.

	$M^a$ ( $\mu_B$ )	$\chi$ ( $10^{-6}$ emu/mol)	LDOS <sup>b</sup> (states/Ry)	$\chi_{\text{Pauli}}$ ( $10^{-6}$ emu/mol)	Ref. 7	$\alpha_d$ This work
Bulk	0.012	285	31.3	74	0.74	0.77
S-I	0.008	190	24.5	58		
Surf	0.006	142	21.8	52	0.50	0.41

<sup>a</sup>Magnetic moments in Bohr magnetons in a field of 0.1 mRy (1.0 mRy) =  $2.35 \times 10^6$  G.

<sup>b</sup>LDOS as taken from Fig. 2 of Ref. 7.

lower than that of the bulk (for a nearly filled  $d$  band). Actually, necessary corrections, which account for charge redistribution do not invalidate this simple picture.

A more quantitative version of this argument is found in calculations by Weinert and Freeman.<sup>7</sup> It has been remarked earlier<sup>7,8</sup> that their calculated Knight shifts for a five-layer slab compare very well with the experimentally observed range of Knight shifts in a small particle. Although their variables probably cannot be compared in detail with the corresponding parameters in our fit, the trends are similar. The total LDOS in Fig. 2 of Ref. 7 in the outer layer is about  $\frac{2}{3}$  that of the central layer, comparable to the value 14.8/24.3 for the surface-to-bulk ratio in Fig. 5(a). In Table V we have reported the enhanced susceptibility as well as the bare Pauli susceptibility, as they can be calculated from Ref. 7 for the central layer and the surface layer of the Pt slab. In each case, we have calculated the corresponding  $\alpha_d$ 's, neglecting the  $s$  contribution of the LDOS at  $E_F$  (Ref. 7) for the bulk and taking it to be equal to 25% of the total LDOS (as calculated by us) at the surface. The enhancements thus obtained are in good agreement with the present results and with our initial assumption that the exchange integral is constant.

### B. The H-covered surface (LTRH)

The diminution of the number of bulklike sites [Fig. 2(b)] upon hydrogen adsorption may have purely geometrical and/or electronic-structure origins. Although effects of hydrogen adsorption on surface reconstruction are known,<sup>28,29</sup> the simultaneous change in LDOS at the surface [Fig. 5(b)] seems to indicate the importance of electronic effects. From our preliminary work (not shown here) on the Pt-particle size dependence of the effect, and neglecting geometric effects, we estimate that the hydrogen coverage affects the electronic structure in at most 1.5 to 2 Pt layers. This seems compatible with the idea that initial adsorption of hydrogen occurs in the threefold and fourfold hollow sites of the (111) [(100)] surfaces.<sup>30–32</sup>

The reduction of the surface LDOS in H-covered Pt, and the associated diminution of the susceptibility (which is amplified by deenhancement effects), are consistent with the observation that hydrogen adsorption removes the magnetization of Ni particles<sup>33,34</sup> [similar effects have been found in surface studies of H/Ni (100) (Ref. 35), CO/Ni (110) (Ref. 36)], and with the theoretical explanation of the photoelectron spectra of hydrogen-covered Pd

surfaces.<sup>37</sup>

In a rigid-band model, the changes in the LDOS can be understood from a mechanism similar to that proposed by Harris and Anderson<sup>38</sup> to explain the extremely low activation for dissociative chemisorption of  $H_2$  on transition metals. The mechanism involves the reverting of  $s$  electrons to the  $d$  band. This will lead to partial filling of the  $d$  holes, diminishing  $D_d$ , and a diminished number of  $s$  electrons, and therefore a (weak) diminution of  $D_s$ , consistent with what is found by comparing Figs. 5(a) and 5(b).

The  $K$  and  $T_1$  values at the surface peak of the H-covered surface coincide with values found by Ansermet for a CO-covered surface.<sup>39</sup> An easy explanation may be found in the fact that in both cases the Fermi level shifts at the very top of the  $d$  band upon chemisorption. At this position in the band, the DOS is very flat so that the effect of CO on magnetic properties is essentially the same as that of H, although the chemisorption bond strengths may be different. It has been observed before<sup>2</sup> that the resonance frequency for the CO-covered surface is in the region found for Pt-carbonyl cluster compounds. A recent  $T_1$  study of the Pt<sub>26</sub> and Pt<sub>38</sub> carbonyls<sup>40</sup> shows a deviation from the Korringa relation for temperatures below 4 K, although relaxation remained rather fast compared to most diamagnetic compounds. This may be related to the paramagnetism detected in these compounds.<sup>41</sup>

### C. The SMSI surface (HTR)

One clear result of the NMR data concerning the SMSI effect is that the back-spillover hypothesis probably is incorrect, as can immediately be seen by comparing data for the SMSI and for the H-covered surface. It is, however, not easy to be more specific, due to the lack of other magnetism-related studies of the effect. As a consequence, we cannot say whether the change in the number of bulklike sites is most likely due to geometrical or to electronic reasons: note that the change in LDOS in the surface region is small on the average, although the data hint at the existence of two environments, with total LDOS of 13.2 and 16 states/Ry atom. The latter value occurs at the maximum of the intensity of the surface peak, indicating that many nuclei are in a nearly "normal surface" environment (in the average sense of the term "surface").

The values found for the surface LDOS exclude significant amounts of ionic or covalent bonding of surface Pt atoms with other species created during the HTR

treatment, but the occurrence of alloying<sup>42</sup> or other metalliclike bonding is not excluded (and perhaps even indicated by the data at 13.2 states/Ry atom).

Indeed, much evidence has been obtained recently from AES (Auger-electron spectroscopy)-XPS (x-ray photoelectron spectroscopy) sputter profiling<sup>43-45</sup> on model catalysts, showing that in group-VIII metals on TiO<sub>2</sub>, a reduced form of titania (TiO<sub>x</sub>) can migrate onto the metal surface. As a result, much of the decrease in chemisorption on TiO<sub>2</sub>-supported Pt upon HTR was attributed to a physical blockage of the surface Pt sites.<sup>46</sup> These results confirm the interpretation of earlier studies by transmission electron microscopy<sup>47</sup> and ESR.<sup>48</sup>

Charge-transfer effects have also been invoked to explain the SMSI state,<sup>49,50</sup> but the experimental evidence for such effects is confusing; some groups claiming no transfer at all,<sup>44,51,52</sup> others small transfers ( $2 \times 10^{-2}$  electrons/Pt-atom),<sup>53</sup> or even important transfers (greater than  $10^{-1}$  electrons/Pt-atom).<sup>54,55</sup> Part of the confusion may be related to intricacies of the interpretation of XPS spectra (see, for instance, the discussion in Ref. 56). Although NMR is only sensitive to the single point in the electron energy spectrum (at the Fermi energy), we still can find some information on the charge transfer (an integral property of the electron spectrum) due to the local character of NMR data, that shows a perfectly normal LDOS for the sites in the interior of the Pt particles. This virtually excludes the occurrence of important charge transfer, but small transfers, mostly "piling up" in the surface region, are compatible with the NMR data.

#### D. Total average susceptibility

From the simultaneous knowledge of  $D_\lambda(E_F)$  and  $\alpha_\lambda$  for the points in Fig. 3(c) [corresponding to the center of the polygons in Fig. 5(a)] it is easy to calculate the total average susceptibility  $\chi_{\text{tot}}$  [ $\chi$  from Eq. (1) plus the diamagnetic contribution] for the "clean" sample. The total susceptibility for different shifts in the line, assuming  $\chi_{\text{dia}} = -30 \times 10^{-6}$  emu/mol,<sup>5</sup> is shown in Fig. 7. It is a simple matter now to deduce the total average susceptibility of our assembly of particles since the NMR intensity curve  $I(s_0)$  gives the probability of finding a nucleus resonating at a given value of  $s_0 = H_0/\nu_0$  [Fig. 2(a)]:

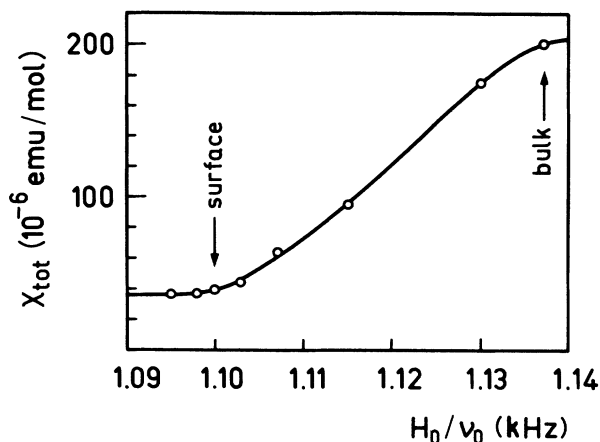


FIG. 7. Total susceptibility (including the diamagnetic contribution) as a function of the position in the resonance line.

$$\langle \chi_{\text{tot}} \rangle = \frac{\int I(s_0) \chi_{\text{tot}}(s_0) ds_0}{\int I(s_0) ds_0} \quad (5)$$

We obtain  $\langle \chi_{\text{tot}} \rangle / \langle \chi_{\text{tot}}^{\text{bulk}} \rangle = 0.6$ . This value is essentially independent of temperature between 10 and 77 K since experimentally no important changes occur in NMR spectra or the Korringa constant in this range. Such a diminution with respect to the bulk value was also found by static susceptibility measurements<sup>57</sup> on particles of approximately the same size as ours, but contrary to what is reported in Ref. 57, we do not find any temperature effect between 10 and 77 K.

*Note added in proof.* R. F. Marzke (private communication) informs us that the lowering of the susceptibility reported in Ref. 43 has not been found in more recent experiments.

#### ACKNOWLEDGMENTS

The catalyst was kindly provided by Professor M. Graetzel [Institut de Chimie Physique, Ecole Polytechnique Fédérale de Lausanne (EPFL)]. We would like to thank I. Rodicio for dispersion measurements and electron microscopy, and Dr. H. Mathieu (Laboratoire de Métallurgie Chimique, EPFL) for XPS measurements.

<sup>1</sup>H. E. Rhodes, Po-Kang Wang, H. T. Stokes, C. P. Slichter, and J. H. Sinfelt, *Phys. Rev. B* **26**, 3559 (1982).

<sup>2</sup>C. D. Makowka, C. P. Slichter, and J. H. Sinfelt, *Phys. Rev. B* **31**, 5663 (1985).

<sup>3</sup>G. C. Carter, L. G. Bennett, and D. J. Kahan, *Progress in Material Science* (Pergamon, New York, 1977), Vol. 20, Pt. I.

<sup>4</sup>Y. Yafet and V. Jaccarino, *Phys. Rev.* **133**, A1630 (1964).

<sup>5</sup>J. P. Bucher and J. J. van der Klink (unpublished).

<sup>6</sup>A. J. Freeman, C. L. Fu, M. Weinert, and S. Ohnishi, *Hyperfine Interact.* **33**, 53 (1987).

<sup>7</sup>M. Weinert and A. J. Freeman, *Phys. Rev. B* **28**, 6262 (1983).

<sup>8</sup>J. J. van der Klink, J. Buttet, and M. Graetzel, *Phys. Rev.* **29**, 6352 (1984).

<sup>9</sup>S. J. Tauster, S. C. Fung, and R. L. Garten, *J. Am. Chem. Soc.*

**100**, 170 (1978).

<sup>10</sup>S. J. Tauster and S. C. Fung, *J. Catal.* **55**, 29 (1978).

<sup>11</sup>F. M. Dautzenberg and H. B. M. Wolters, *J. Catal.* **51**, 26 (1978).

<sup>12</sup>G. A. Martin, R. Dutartre, and J. A. Dalmon, *React. Kinet. Catal. Lett.* **16**, 329 (1981).

<sup>13</sup>K. Kunimori, Y. Ikeda, M. Soma, and T. Uchijima, *J. Catal.* **79**, 185 (1983).

<sup>14</sup>R. Lambert, *Thin Solid Films* **128**, L29 (1985).

<sup>15</sup>J. P. Bucher, J. Buttet, J. J. van der Klink, M. Graetzel, E. Newson, and T. B. Truong, *J. Mol. Catal.* **43**, 213 (1987).

<sup>16</sup>G. H. Ayres, *Anal. Chem.* **25**, 1622 (1953).

<sup>17</sup>M. J. Yacaman and J. M. Dominguez, *Surf. Sci.* **87**, L263 (1979); M. L. Sattler and P. N. Ross, *Ultramicrosc.* **20**, 21

- (1986).
- <sup>18</sup>*Metal-Support and Metal-Additive Effects in Catalysis*, edited by B. Imelik *et al.* (Elsevier, Amsterdam, 1982).
- <sup>19</sup>A. V. Zelewsky, *Helv. Chim. Acta* **51**, 803 (1968).
- <sup>20</sup>C. Froidevaux and M. Weger, *Phys. Rev. Lett.* **12**, 123 (1964).
- <sup>21</sup>J. Koringa, *Physica* **16**, 601 (1950).
- <sup>22</sup>M. Shaham, U. El Hanany, and D. Zamir, *Phys. Rev.* **17**, 3513 (1978).
- <sup>23</sup>R. W. Shaw and W. W. Warren, *Phys. Rev.* **3**, 1562 (1971).
- <sup>24</sup>J. P. Bucher and J. J. van der Klink, *Solid State Commun.* **65**, 27 (1988).
- <sup>25</sup>J. F. Janak, *Phys. Rev.* **16**, 255 (1977).
- <sup>26</sup>B. Morawek and A. J. Renouprez, *Surf. Sci.* **106**, 35 (1981).
- <sup>27</sup>S. N. Khanna, J. P. Bucher, J. Buttet, and F. Cyrot-Lackmann, *Surf. Sci.* **127**, 165 (1983).
- <sup>28</sup>P. R. Norton, J. A. Davies, D. P. Jackson, and N. Matsunami, *Surf. Sci.* **85**, 269 (1979).
- <sup>29</sup>This ability of hydrogen to restore the bulk structure of surfaces has also been established for Pt clusters in *Y* zeolites; see, for instance, P. Gallezot, A. I. Bienenstock, and M. Boudart, *Nouv. J. Chim.* **2**, 263 (1978); B. Morawek, G. Clugnet, and A. J. Renouprez, *Surf. Sci.* **81**, L631 (1979).
- <sup>30</sup>A. M. Baro, H. Ibach, and H. D. Bruchmann, *Surf. Sci.* **88**, 384 (1979).
- <sup>31</sup>P. J. Feibelman and D. R. Hamann, *Surf. Sci.* **182**, 411 (1987).
- <sup>32</sup>D. Tománek, S. G. Louie, and C.-T. Chan, *Phys. Rev. Lett.* **57**, 2594 (1986).
- <sup>33</sup>G. A. Martin and B. Imelik, *Surf. Sci.* **42**, 157 (1974).
- <sup>34</sup>P. W. Selwood, *Chemisorption and Magnetization* (Academic, New York, 1975), and references therein.
- <sup>35</sup>M. Landolt and M. Campagna, *Phys. Rev. Lett.* **39**, 568 (1977).
- <sup>36</sup>C. S. Feigerle, A. Seiler, J. L. Pena, R. J. Celotta, and D. T. Pierce, *Phys. Rev. Lett.* **56**, 2207 (1986).
- <sup>37</sup>S. G. Louie, *Phys. Rev. Lett.* **42**, 476 (1979).
- <sup>38</sup>J. Harris and S. Anderson, *Phys. Rev. Lett.* **55**, 1583 (1985).
- <sup>39</sup>J.-P. Ansermet, Ph.D. thesis, University of Illinois, 1985.
- <sup>40</sup>B. J. Pronk, H. B. Brom, A. Ceriotti, and G. Longoni, *Solid State Commun.* **64**, 7 (1987).
- <sup>41</sup>B. J. Pronk, H. B. Brom, L. J. de Jongh, G. Longoni, and A. Ceriotti, *Solid State Commun.* **59**, 349 (1986).
- <sup>42</sup>B. C. Beard and P. N. Ross, *J. Phys. Chem.* **90**, 6811 (1986).
- <sup>43</sup>G. L. Haller, V. E. Henrich, M. McMillan, D. E. Resasco, H. R. Sadeghi, and S. Sakellson, in *Proceedings of the Eighth International Congress on Catalysis, Berlin, 1984* (Dechema Verlag, Berlin, 1984), Vol. V, p. 135.
- <sup>44</sup>D. N. Belton, Y.-M. Sun, and J. M. White, *J. Phys. Chem.* **88**, 1690 (1984).
- <sup>45</sup>Y.-M. Sun, D. N. Belton, and J. M. White, *J. Phys. Chem.* **90**, 5178 (1986).
- <sup>46</sup>C. S. Ko and R. J. Gorte, *Surf. Sci.* **155**, 296 (1985).
- <sup>47</sup>R. T. K. Baker, E. B. Prestridge, and R. L. Garten, *J. Catal.* **56**, 390 (1979).
- <sup>48</sup>T. Huizinga and R. Prins, *J. Phys. Chem.* **85**, 2156 (1981).
- <sup>49</sup>J. A. Horsley, *J. Am. Chem. Soc.* **101**, 2870 (1979).
- <sup>50</sup>S. J. Tauster, S. C. Fung, R. T. K. Baker, and J. A. Horsley, *Science* **211**, 1121 (1981).
- <sup>51</sup>T. Huizinga and R. Prins, in *Metal-Support and Metal-Additive Effects in Catalysis*, edited by B. Imelik *et al.* (Elsevier, Amsterdam, 1982), p. 11.
- <sup>52</sup>B. H. Chen and J. M. White, *J. Phys. Chem.* **86**, 3534 (1982).
- <sup>53</sup>D. R. Short, A. N. Mansour, J. W. Cook, D. E. Sayers, and J. R. Katzer, *J. Catal.* **82**, 299 (1983).
- <sup>54</sup>M. K. Bahl, S. C. Tsai, and Y. W. Chung, *Phys. Rev.* **21**, 1344 (1980).
- <sup>55</sup>S. C. Fung, *J. Catal.* **76**, 225 (1982).
- <sup>56</sup>A. Masson, B. Bellamy, Y. Hadj Romdhane, M. Che, H. Roulet, and G. Dufour, *Surf. Sci.* **173**, 479 (1986).
- <sup>57</sup>R. F. Marzke, W. S. Glausinger, and M. Bayard, *Solid State Commun.* **18**, 1025 (1976).
- <sup>58</sup>A. M. Clogston, V. Jaccarino, and Y. Yafet, *Phys. Rev.* **134**, A650 (1964).
- <sup>59</sup>D. A. Papaconstantopoulos, *Calculated Electronic Properties of Metals* (Pergamon, New York, 1986).
- <sup>60</sup>A. H. Mac Donald, J. M. Daams, S. H. Vosko, and D. D. Koelling, *Phys. Rev.* **23**, 6377 (1981).